Influence of fluctuating supply on the emplacement dynamics of channelized lava flows

Simone Tarquini[1*] and Mattia de' Michieli Vitturi[1]

[1]*Istituto Nazionale di Geofisica e Vulcanologia, Sezione di Pisa, Italy*

The final publication is available at www.springerlink.com (*http://link.springer.com/article/10.1007/s00445-014-0801-2)*

Pre-print version of the following paper:
Tarquini S, de' Michieli Vitturi M (2014) Influence of fluctuating supply on the emplacement dynamics of channelized lava flows – Bulletin of Volcanology, 76:801. *DOI:10.1007/s00445-014-0801-2*

Keywords: lava flows; emplacement dynamics; lava flow modeling; Mount Etna

Editorial responsibility: MR Patrick

Abstract

The evolution of lava flows emplaced on Mount Etna (Italy) in September 2004 is examined in detail through the analysis of morphometric measurements of flow units. The growth of the main channelized flow is consistent with a layering of lava blankets which maintains the initial geometry of the channel (although levees are widened and raised), and is here explicitly related to the repeated overflow of lava pulses. A simple analytical model is introduced describing the evolution of the flow level in a channelized flow unit fed by a fluctuating supply. The model, named FLOWPULSE, shows that a fluctuation in the velocity of lava extrusion at the vent triggers the formation of pulses which become increasingly high the farther they are from the vent, and are invariably destined to overflow within a given distance. The FLOWPULSE simulations are in accordance with the observed morphology, characterized by a very flat initial profile followed by a massive increase in flow unit cross-section area between 600 and 700 m downflow. The modeled emplacement dynamics provides also an explanation for the observed substantial "loss" of the original flowing mass with increasing distance from the vent.

Introduction

The lava discharge rate during effusive eruptions is often unsteady at a variety of time scales, and as increasingly powerful observation techniques are applied in studying volcanoes, this unsteadiness becomes increasingly apparent (e.g. Lautze et al. 2004; Bailey et al. 2006; James et al. 2010). A variable supply rate has already been invoked to explain the formation of pulses of lava along channelized flows by several authors (James et al. 2007; Favalli et al. 2010; Wadge et al. 2012). In spite of the above evidence, until recently, lava flow modeling has focused almost exclusively on steady supply conditions (e.g. Robertson and Kerr 2012; Filippucci et al. 2013), with only minor modifications considered (e.g. Baloga 1987). As a result, the implications of a transient lava discharge rate on lava flow dynamics have only been marginally explored so far.

In the following, a suite of detailed morphometric measurements of an active lava flow at Mount Etna is used to infer a systematic growth mechanism for channelized lava flow units. Afterwards, we introduced a simple model of fluctuating supply, named FLOWPULSE, that reproduces the formation of pulses in a channelized flow and correlates the occurrence of pulse overflow with a given distance from the vent, thus providing quantitative support for the inferred emplacement dynamics.

[*] corresponding author at Istituto Nazionale di Geofisica e Vulcanologia, Sezione di Pisa, via U. della Faggiola 32, 56126 Pisa, Italy. Tel +39 050 8311932 email: tarquini@pi.ingv.it.

Evolution of the September 2004 lava flows at Etna

Measurements

On 16th September 2004, from 7:00 to 8:30 a.m. LT, a LIDAR survey was carried out at Mount Etna while the 2004-2005 flank eruption was discharging lava onto the Eastern flank of the volcano from two separate vents (Mazzarini et al. 2005) (Figs. 1-3). Burton et al. (2005) showed a thermal map acquired on 15th September (between 6:15 and 6:35 LT) for the same effusive activity. The thermal map (Fig. 1c), along with a visual image of the eruptive scenario at 7:30 LT on the same day (Fig. 2), shows that the overflow units 1.1 and 1.2 (Fig. 1b) were absent on 15th September. Therefore, the overflow "ɪ " is younger than ~24 h (Fig. 1).

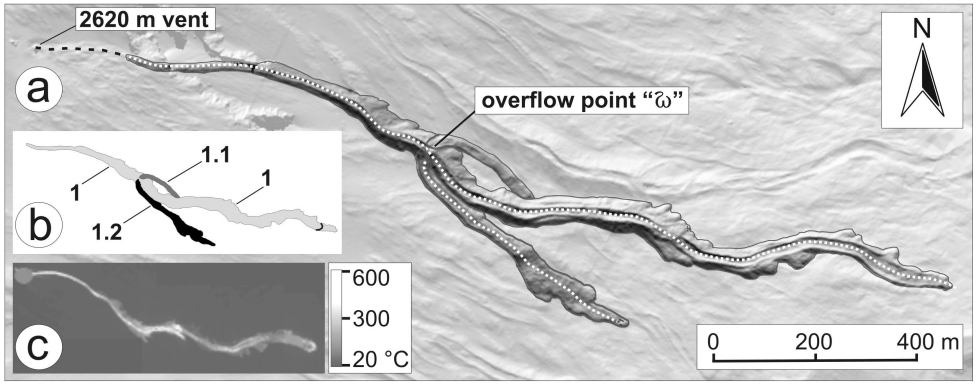

Fig. 1. Lava flows formed from vent at 2620 m above sea level. a) flow units are highlighted by a darker shadowing; white dotted lines are the axes of flow units (f.u.) 1 and 1.2 used to derive the morphometric measurements of Fig. 4; the black dashed line is the very proximal section of the main channel (~180 m-long) which has no morphological evidence at DEM resolution (2 m) and thus was not mapped through the morphology-based methods of Mazzarini et al. (2005) and Tarquini et al. (2012), and so this determines the shift of the values along abscissas in Fig. 4. b) sketch with flow unit labels. c) Thermal map, with related legend, modified after Burton et al. (2005); the map was derived by merging several un-rectified thermal pictures, which explains distortion in plan view. The front of f.u. 1 advanced an additional 80-90 m between the two surveys (notice the mark near the front of the flow in frame b).

Favalli et al. (2009), by processing a time series of strips from the same LIDAR survey, discovered that lava pulses were advancing downhill along the active channelized flow units. They based their analysis on elevation-difference maps, which reveal the morphological modifications that occurred during the intervals between acquisition of the considered strips. Pulses are revealed by a characteristic elevation-difference pattern along the channel (an alternation of maxima and minima). Favalli et al. (2009) further highlighted that the main flow unit originating from the vent at 2620 m above sea level since 10th September (1 in Fig. 1b) was discharging all its lava supply into the overflow unit 1.2, while the rest of the main flow unit 1 (downhill from the overflow point "ɪ ") and the other overflow unit 1.1 were unchanging in thickness and essentially inactive.

By processing a series of hyperspectral data acquired by NASA's Earth Observing-1 Hyperion imaging spectrometer, Wright et al. (2010) analyzed the emplacement of the same flow field. These authors showed 3 images acquired on the nights of 12, 14 and 16 September 2004. In Fig. 3 we consider their 14 and 16 September images as taken from their Fig. 2 (Wright et al. 2010). Although the views are not strictly at the nadir and are taken from slightly different angles, the planimetric distortion is quite low and allows image superposition to detect changes in the flow field. Fig. 3b confirms that on 16 September flow unit 1.2 was active, while the portion of the flow unit 1 downhill from the overflow point ɪ was no longer being fed.

By using the morphometric technique described by Tarquini et al. (2012), the morphology of the active overflow unit (1.2) is compared with that of the parent flow unit 1 (Fig. 4). Interestingly, in spite of the striking difference in overall height of the flow units, the widths of the two channels and the outward slopes are very similar. The outward slope is essentially governed by the repose angle of talus, and it is not surprising that both accumulated material (lava fragments) and slope turn out to be similar from unit to unit; the close similarity of the width of the two channels, however, has more interesting implications which are discussed in the next section.

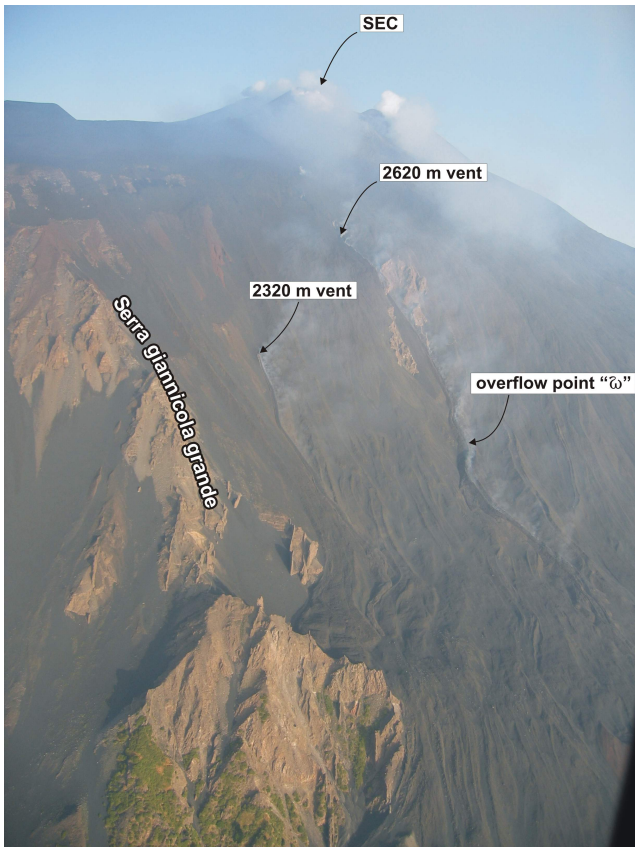

Fig. 2. A picture taken at 7:30 LT on 15 September 2004 during an overflight over the Valle del Bove, where two vents at 2620 and 2320 m above sea level (feeding two "smoking" flow units) were simultaneously active. The point where the overflow will occur is labeled. SEC = south east crater. Photo courtesy of Sonia Calvari.

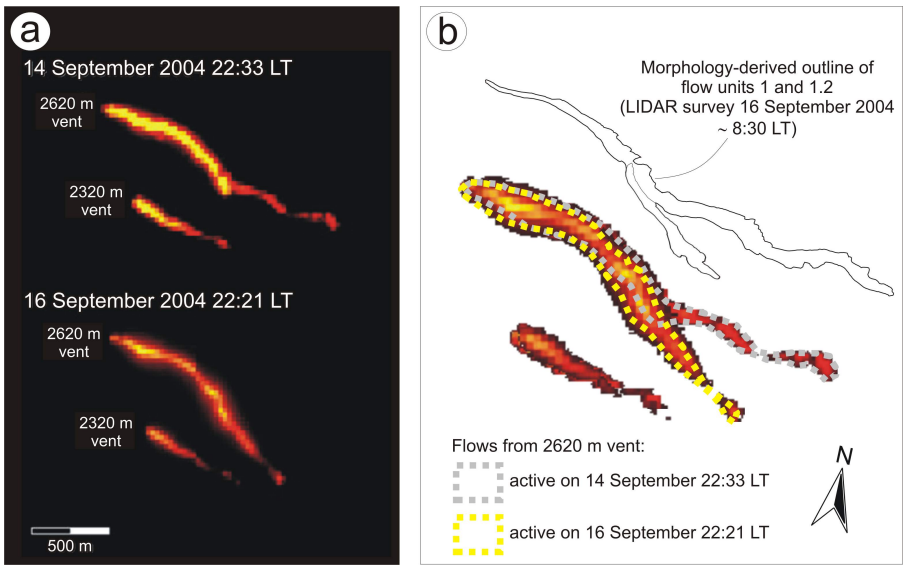

Fig. 3. Analysis of the NASA's Hyperion hyperspectral images. a) false color images of the Etna flow field active on 12 and 14 September 2004 (modified after Wright et al., 2010); red to yellow is for increasingly hot pixels which indicate an active, strongly radiating lava flow; black is for the "cold" background. b) Hot pixels of the 16 September scene are superposed to hot pixels of the 14 September scene; a comparison with the outline of flow units obtained from the 16 September LIDAR survey (rotated clockwise by ~12° with respect to Fig. 1) highlights a fairly low planimetric distortion and the confluence of the whole lava supply in flow unit 1.2 on 16 September. This outcome supports the temporal evolution of the flows discussed in the main text.

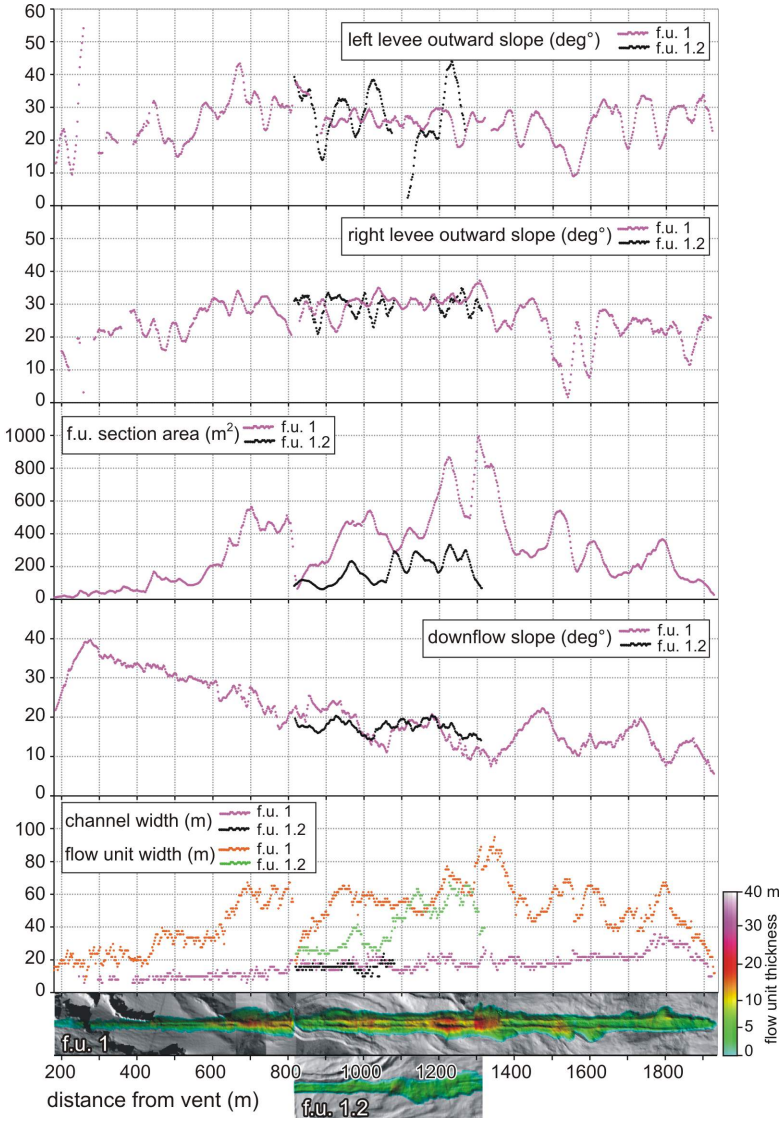

Fig. 4. Comparison between the morphometry of flow units (f.u.) 1 and 1.2. Data for f.u. 1 are taken from Tarquini et al. (2012); see the same reference for details about the method, based on a mathematical processing of elevation profiles traced orthogonal to the flow axis. See caption of Fig. 1 for the shift along abscissas. To support the interpretation of plots, shaded relief images of both flow units obtained in an along-the-flow coordinate system are aligned with the plots. Colors show the thickness of the flow units (Tarquini et al., 2012).

The lava output rate for the considered effusive activity has been estimated at different times by different authors using different methods: Burton et al. (2005), through field measurements, estimated between 2.3 and 4.1 m^3sec^{-1} for the first 90 days of activity; Mazzarini et al. (2005) calculated by simple DEM subtraction 2.2 ± 0.8 m^3sec^{-1} for the flows sourced from the vent at 2620 m asl (Fig. 1) in the first six days; Harris et al. (2007) reported a channel-based measurement of 2-4 m^3sec^{-1} ~5 meters downflow from the vent; and James et al. (2007) reported an independent channel-based measurement "near the vents" of 4-5 m^3sec^{-1}. By applying the DEM-difference-based method described by Favalli et al. (2010) to the 2004 LIDAR dataset, we calculated 9 +/-1 x 10^3 m^3 for the volume of the lava emplaced over the period (76 minutes) between the time of acquisition of the two LIDAR strips (see Favalli et al. 2009; 2010 for details). The two strips overlap (approximately) only over the second half of the active flow, and therefore we missed any possible volume increase which occurred in the first half of the feeding channel from the vent downhill (see also Favalli et al. 2009). To a first approximation, assuming a grossly equivalent volume increase over the two flow segments (first and second halves), the lava supply rate for the whole active flow can be estimated as ~4 m^3 sec^{-1} at the time of the LIDAR survey.

The morphometric technique presented by Tarquini et al. (2012) can be also used to obtain the volume of flow units. This is done by calculating the integral over the flow unit thickness map (see the bottom of Fig. 4). This method is used to calculate the cumulative volume of flow units (f.u.) 1.1 and 1.2, which can be used, in turn (coupled with the estimated effusion rate), to estimate the time of occurrence of the overflow "I ". The total volume constituting f.u. 1.1 and 1.2 is ~90 × 10^3 m^3, implying that the overflow started between 12.5 and 6.25 hours before the LIDAR survey (considering a supply rate of 2 and 4 m^3 sec^{-1} respectively). This emplacement duration is consistent with the time constraint for the onset of the overflow "I " fixed by the picture in Fig. 2 (i.e. not earlier than 24 h before the LIDAR survey).

Analysis of the DEM difference maps discussed by Favalli et al. (2010) allows an estimation of the velocity of lava pulses. The ratio between the length along the flow of the maxima (i.e. increase in flow level) over the time interval between the acquisition of the two considered "snapshots of the topography", provides a measure of the pulse velocity. Fig. 9 in Favalli et al. (2009) shows that the length of the large pulse halfway along the overflow unit 1.2 (at about 1 km downhill from the vent) is approximately 150-200 m; by considering the time interval of 76 minutes between the two LIDAR strips, we estimate a pulse velocity of 0.032-0.043 m sec^{-1}.

Growth mechanism

The overall consistency of all the available measurements of the supply rate leads us to infer that the average supply rate, calculated over a duration longer than the pulse period, was grossly constant (i.e. characterized by an analogous reiteration of similar pulses), at least during the first days of the effusion imaged by the 2004 LIDAR. Within this inference, the initial sector of the overflow unit 1.2 (flanking flow unit 1) is considered a proxy of what should have been the adjacent sector of the parent flow unit 1 at a similar age. According to this view, the channel width and slope of the levees, established in the early formation of the channel (Hulme 1974; Favalli et al. 2010), did not change during the subsequent growth of the flow unit, which increased the area of the flow unit section by an impressive factor of 3-4 (Figs. 4 – 5).

If the supply rate was not changed (i.e. the system was fed by similar pulses), the depth of the lava flowing on 15th September through the section s_1 (flow unit 1) and the depth of the lava which was flowing through the section $s_{1.2}$ (flow unit 1.2) at the time of the LIDAR survey (Fig. 5a), must have been the same during the same lava flux. This is because, after having traveled along the same feeding channel (Fig. 5a) under the same supply conditions (with the lava in similar thermo-rheological conditions), the same amount of lava enters channels having similar width and slope (as inferred from Figs. 4 – 5), and will therefore be accommodated in a flow having the same thickness. Hence, the channels in flow units 1 and 1.2 should be equally deep (Fig. 5b), which adds a further geometrical constraint addressed later in the discussion section.

It is inferred here that the mechanism of growth for levees already present is a repeated overflow triggered by the observed pulsating supply. A single episode of levee building sustained by the overflow of a pulse has been already observed and documented in detail by James et al. (2007). If this mechanism is the sole levee building process, then the systematic reiteration of similar overflows is responsible for the piling-up of up to 20 m of lava over both the levees in five days (overflow levees, Sparks et al. 1976).

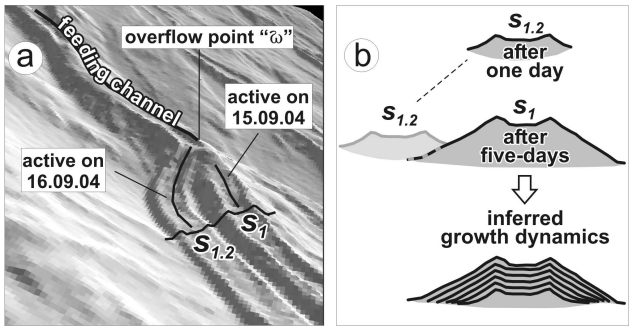

Fig. 5. Time-evolution analysis of flow units. a) perspective view of the channels near the overflow point I , the sections s_1 an $s_{1.2}$ over the respective flow units 1 and 1.2 are shown. b) sketch of the inferred growth mechanism.

Modelling and results

A simple model is introduced to describe kinematically the movement of lava in a channel. The Model, named FLOWPULSE, is based on the discretization of the flowing lava in what we term parcels, which are increments or volumes of lava. Parcels are emitted from the vent with a certain initial velocity, and flow into an established channel with a given geometry (Fig. 6a). Parcels are emitted at a specified frequency $\mathcal{3}$ and, as the same mass is attributed to each parcel, the frequency $\mathcal{3}$ is directly proportional to the supply rate. After emission, parcels move unimpeded by any other parcels (as they would be in FLOWGO (Harris and Rowland 2001)).

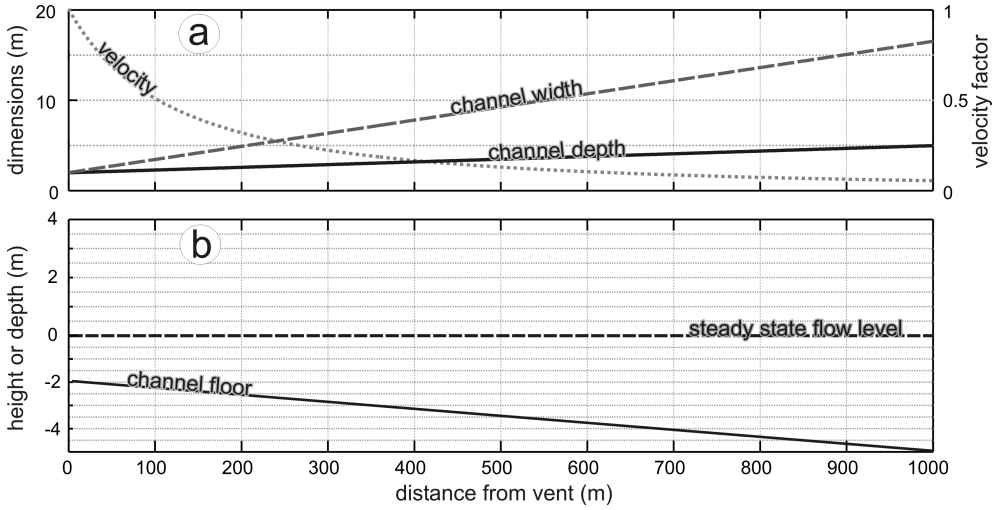

Fig. 6. Channel geometry and flow velocity at steady flux rate. a) prescribed depth and width and consequent law for the velocity decay; the initial width of the channel is 2 m (common value for similar cases at Etna), then the width increases according to a linear regression of data plotted in Fig. 4; the initial depth of the channel has been set to 2 m, considering that the thickness of channel-contained pulses reaches similar values in very proximal sections (Favalli et al., 2009; 2010), then the depth increases, gently and linearly, up to 5 m at 1 km downhill (see also Fig. 6b), accounting for measurements shown in Tarquini et al., 2012. The initial maximum velocity has been set to 1 m/sec, close to the 0.7 m/sec reported by Harris et al., 2007, with a consequent maximum supply rate of 4 m^3/sec (as previously found). b) In this scheme the reference flow level in steady state conditions is set as the zero value (abscissas), and the increasing flow depth (the same as in the panel above) is therefore shown as a deepening of the channel floor; the same scheme is used in the following Figs. 7-9 (slightly modified) and Fig. 10 to better visualize changes in flow level introduced by the transient condition.

The reference solution is obtained assuming a constant emission frequency ϶, i.e. a constant flow rate (as in Tallarico and Dragoni 1999; 2000; Harris and Rowland 2001). In this condition the velocity of flowing lava strongly decreases with increasing distance from the vent (Fig. 6a) as a consequence of the increasing flow depth (Fig. 6b) and channel width. A similar strong decrease in flow velocity with distance from the vent is commonly observed in real lava flows (e.g. Naranjo et al. 1992). Note that under steady flow conditions the velocity of lava at 1 km downhill from the vent provided by the model is about 0.05 m sec^{-1} for an initial velocity of 1 m sec^{-1} (Fig. 6a, see figure caption for further details), which compares well with the velocity of the pulse at about 1 km downflow from the vent measured above on the flow unit 1.2 (0.032 – 0.043 m sec^{-1}).

In reporting observations made at the proximal section of channelized lava flows at Mount Etna, several authors described fluctuations either in lava velocity (e.g. Guest et al. 1987; Harris et al. 2005; Bailey et al. 2006), in flow level (e.g. Guest et al. 1987; James et al. 2007), or in supply rate (e.g. Frazzetta and Romano 1984). To account for similar changes, the supply rate is varied, and parcels are emitted from the vent at an initial velocity which varies between two extreme values according to a sinusoidal law with period *T*. The parameter a_v expresses the velocity range between the maximum and minimum initial velocities (as a percentage of the maximum velocity), and characterizes the amplitude of the velocity fluctuation. After emission, the velocity of each parcel continues to decrease according to the above relationship (Fig. 6a).

For a constant frequency *϶* of parcel emission (i.e. for a given supply rate) a higher initial velocity results in a lower abundance of parcels per unit length along the flow, which means a lower mass per unit length and hence a lower flow depth *fd* (assuming constant lava properties, including density, see Fig. 7). In our simulations, to keep the flow height at vent constant when the initial velocity of parcels varies, the frequency *϶* of parcel emission is also varied, introducing the variation in supply rate (Fig. 8a).

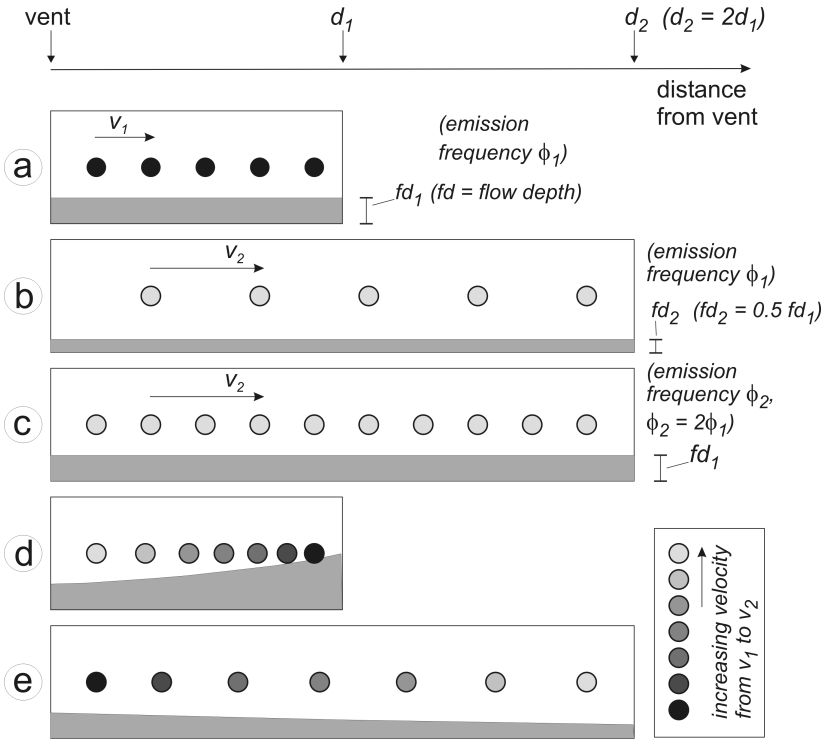

Fig. 7. Simplified sketch describing the effects of the velocity of parcels and the frequency of parcel emission on the flow depth. Parcels are represented by light gray to black circles, the corresponding flow is represented in gray. a) – c) steady supply with different input settings of the model. In case a) the first parcel emitted reaches the distance d_1 in the given time frame f, while in cases b) and c) the first parcel emitted reaches the distance d_2 in the same time. d) – e) variable supply. In d) the velocity of emission varies between v_1 and v_2, while the emission frequency varies synchronously between ϕ_1 and ϕ_2 (variable supply), resulting in an increasing density of parcels (and hence increasing flow depth) with distance from the vent. In e) the velocity of emission varies between v_2 and v_1, while the emission frequency varies synchronously between ϕ_2 and ϕ_1, resulting in a decreasing density of parcels (and hence decreasing flow depth) with distance from the vent. The hue of circles indicate increasing initial velocity from black to light gray. This sketch stimulates a comparison of FLOWPULSE with the theory of kinematic waves (Baloga 1987).

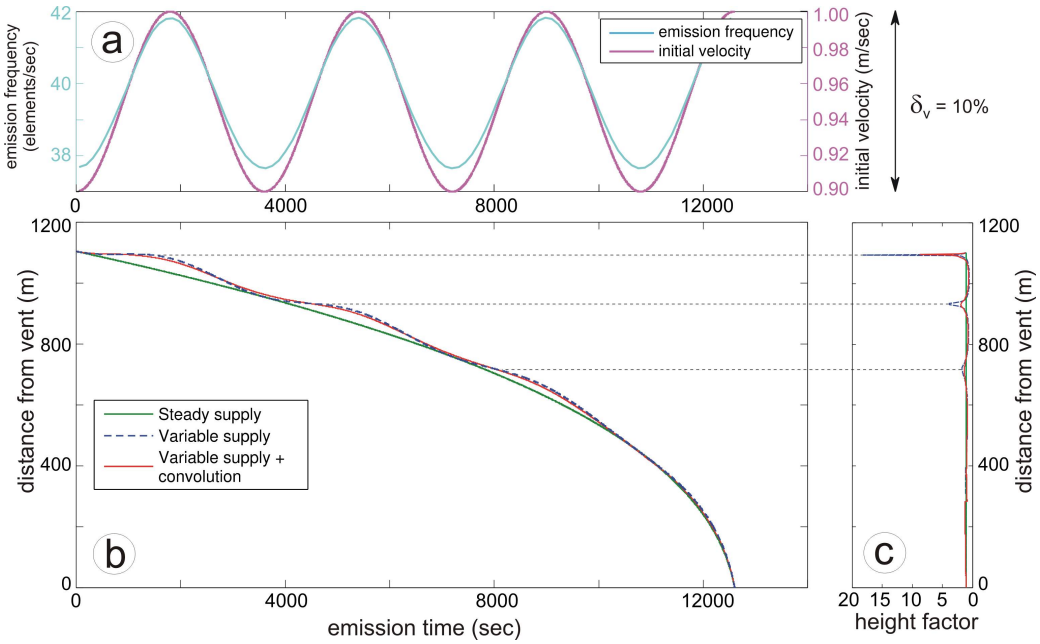

Fig. 8. Model output for a_v = 10%. a) sinusoidal velocity and frequency of parcel emissions at the vent. b) distance attained down-channel by parcels versus time of emission; notice the effect of the fluctuation, which concentrates the parcels at given distances. c) pulses height/depth over the steady state solution versus distance from the vent: thin dashed lines show that peak values in (c) (i.e. pulses) match relative minima (in absolute value) of the derivative of the curves in (b).

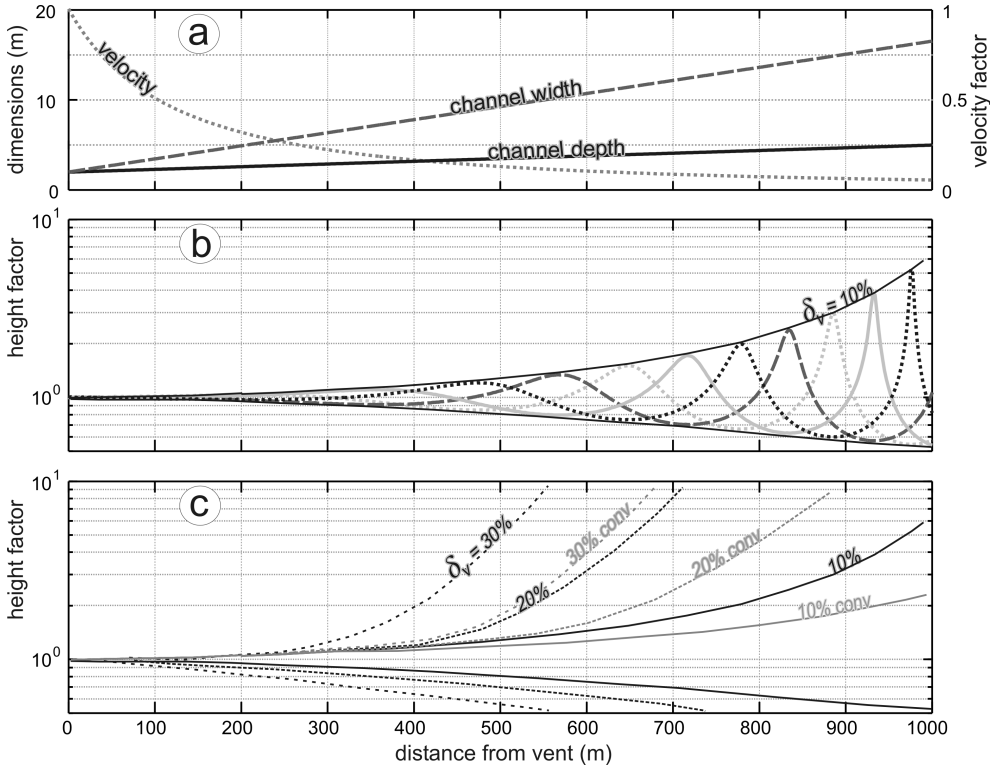

Fig. 9. Model outputs. a) Channel geometry and flow velocity decline versus distance from the vent. b) Black solid lines: envelope of the maximum height of the pulses and of the maximum channel drainage (minimum height) obtained for a_v = 10%. Gray/dashed lines: down-channel flow elevation profiles versus distance from the vent; the four solutions are spaced in time by $T/4$. The elevation is shown as a height factor with respect to the steady state flow level, which equals channel depth in (a). c) Envelopes of maximum heights and minimum drainage reached for a_v = 10%, 20% and 30%, with and without applying a convolution kernel (conv). ("elements/sec" represents “parcels/sec”)

Following the introduction of the fluctuation (in both velocity and frequency), the concentration of parcels along the channel varies with respect to the steady supply condition, because faster parcels tend to overcome slower ones, which were emitted before (Fig. 8b-c). This mechanism weakens the assumption of unimpeded flow, and it would therefore appear that interaction between parcels is promoted. This effect is reproduced in the model by a convolution kernel mimicking a re-distribution of the momentum among parcels emitted within a given time interval (0.5 T) and resulting in a smoothing of their velocity (Fig. 8b – c). Analytical details of the model are provided in the appendix. Fig. 9b shows the results obtained assuming fluctuations in emissions with period T = 1h (as observed by James et al. 2007) and amplitude a_v = 10%. Fig. 9c further shows the model outputs obtained with or without the activation of the convolution kernel, and for different a_v values.

Fig. 10 shows that if the a_v value is relatively large, parcels actually do overtake each other within the distance considered in the plot (Fig. 10b). As a result, the continuity of the flow level is broken and pulses split into two sub-pulses (Fig. 10c). Sub-pulses are separated by a gap which increases downflow (Fig. 10c), implying that the front sub-pulse is faster than the rear sub-pulse. For the same reason, further downflow a front sub-pulse would reach and eventually overtake the rear sub-pulse formed from the pulse which was originally in front of it. Despite this, it is important to highlight that, according to our simulations, far before the onset of splitting or overtaking, pulses have largely exceeded the height of levees (Figs. 8-10) and would therefore have extensively overflowed the channel. We recall that the process of overflow out of the channel is not implemented in the current model, and therefore the interpretation of the post-overflow dynamics of pulses should be made with caution, if at all (as discussed in the next section).

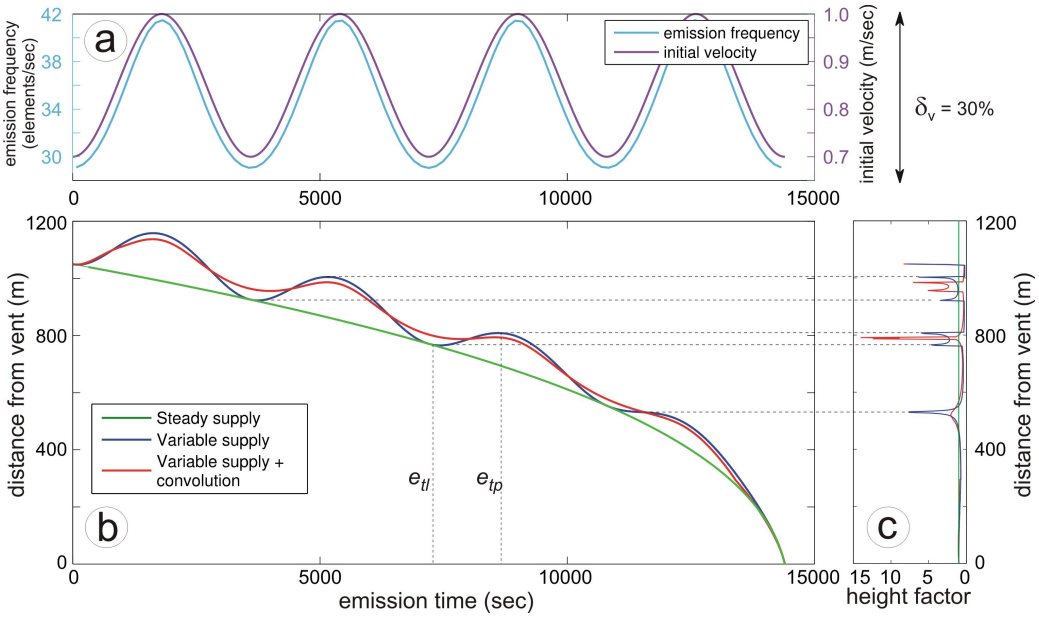

Fig. 10. Model output for a_v = 30%. a) sinusoidal velocity and frequency of parcel emissions at the vent. b) distance attained down-channel by parcels versus time of emission. c) pulses height/depth over the steady state solution versus distance from the vent: horizontal thin dashed lines show that peak values in (c) (i.e. pulses) match relative minima (in absolute value) of the derivative of the curves in (b). To visualize the overtake process between parcels, note the vertical thin dashed lines which highlight the position of the parcel (or element) e_{tp}, emitted at time ~ 8500 sec (during a peak emission velocity) and the position of the parcel e_{tl} emitted before at time ~ 7200 sec (during a low emission velocity). At the end of the simulation e_{tp} already overcame 800 m downflow from the vent (follow the horizontal dashed lines), while e_{tl} is several tens of meters behind.

Discussion

Our model, to some extent, is similar to the one of Baloga (1987), which uses kinematic waves to describe lava flows. Nevertheless, FLOWPULSE does not share the same mathematics, being based on discrete computational elements (the "parcels" of lava) as opposed to the continuous function of the kinematic waves of Baloga (1987). In the model of Baloga (1987) the progression downhill of a nonlinear kinematic wave promotes overtaking of slower parts of the wave by faster ones, and finally a singularity in the solution with infinite slope is generated, resulting in a so called breaking point. As stated by Baloga (1987), the kinematic wave beyond the inner breaking point has no physical meaning. In contrast, overtaking of one parcel by another is not a problem in FLOWPULSE, where, from a mathematical point of view, parcels (specific elements) are free to overtake each other. We note here that the “free overtaking rule” is consistent with behavior of real lava flows, as highlighted later in the discussion.

Simulation results show that a fluctuation in the velocity of extrusion (i.e. in lava supply rate) tends to produce, in a channelized flow, an increasingly high wave (or pulse) as the distance from the vent increases. Each pulse is followed by a sector of increasingly depressed flow.

The rising wave with distance revealed by the simulations can explain the observed pulses in actual channelized flows at Mount Etna (James et al. 2007; Favalli et al. 2009, 2010). The increasing height of the waves, i.e. the modeled lava pulses, can explain the mechanism of growth of the levees, with pulses overwhelming the channel capacity at a given distance and causing lava rubble to cascade over both levees as shown by James et al. (2007).

At what distance from the vent will a pulse overflow? It is a common observation that a channelized lava flow can sustain significant superelevation above the levee before beginning to overflow. This is principally due to the viscosity of lava and to the width of the tops of the levees. Favalli et al. (2010) monitored, for a few hours, the elevation profile along a transect orthogonal to the flow direction during the emplacement of a channelized, pulsating flow unit at Mt Etna at one stage in the 2006 eruption (about 1 km downhill from the relative vent). Their Fig. 8 (Favalli et al. 2010), shows that the left-hand levee sustained at least 1.5 m of superelevation above the top of the levee. It can be presumed that the maximum sustained superelevation will not be a constant value throughout the entire length of a flow unit (e.g. because the lava viscosity generally increases with distance from the vent). Nevertheless, as a first approximation, we assume here that 1.5 m is a constant threshold value beyond which overflow is triggered. The steady-state level (i.e. with steady lava supply) will not necessarily coincide with the height of the top of the levees, but here it is assumed that they coincide.

Within the above assumptions, Fig. 11 plots the maximum flow superelevation above the steady state flow level against the downflow distance where overflow occurs. As an example, overflow will occur between 450 and 700 m downhill from the vent for a_v = 30% and 10% respectively, convolution kernel active. This result matches the very flat initial profile of the main flow unit (Figs. 4, 11b), with a first relevant peak observed at 450 m from the vent, while from 600 to 700 m the growth becomes large, increasing the cross-sectional area by a factor of 3 over ~100 m. A break in slope has been invoked as one of the main accelerators of flow unit growth dynamics, especially in distal sectors (e.g. Tarquini et al. 2012), but Fig. 11b highlights a broadly linear decrease in slope, with only minor variations between 600 and 850 m, suggesting that the growth could instead have been promoted by recurring pulse overflows.

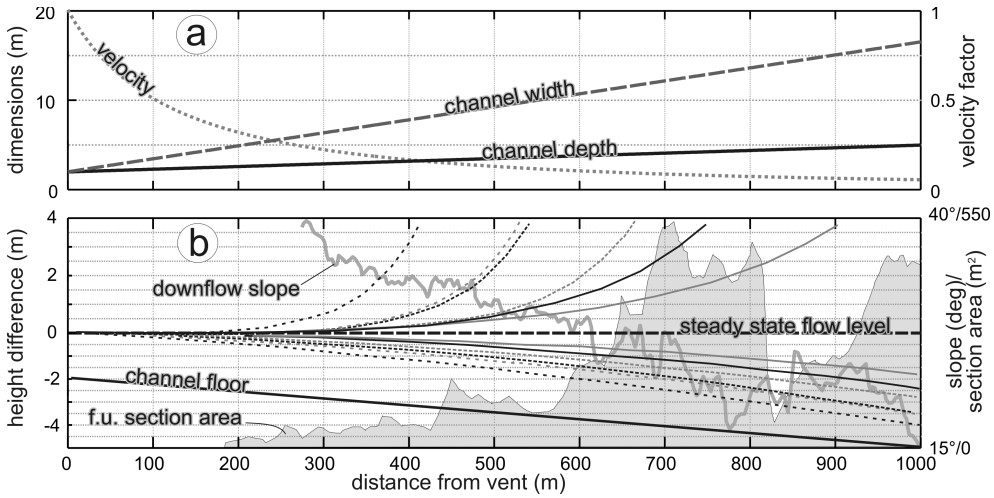

Fig. 11. Model outputs compared to flow unit morphology. a) Channel geometry and flow velocity decline versus distance from the vent. b) modeled pulse superelevation and channel drainage (as height difference between transient and steady flow levels) compared with actual flow unit section area and downflow slope. A few meters after 800 m the section area seems to decrease suddenly. But this is an artifact due to the superposition of the two overflow units 1.1 and 1.2 over the morphology of f.u. 1 which buried the lower part of the main flow hampering its detection (through the morphometric method of Tarquini et al., 2012). When the morphological perturbation disappears (at about 950 m), the full section area is detected again, and the value at 800 m is recovered (see also Fig. 4). The legend for the pulse height envelopes is as in Fig. 8).

Fig. 10 shows that, in theory, pulses originated according to the modeled mechanism, after growing to a maximum elevation, would eventually evolve according to a complex dynamic which includes splitting of pulses and, at greater distance (beyond the domain shown), overtaking of slower-moving sub-pulses by the faster-moving ones. As already stated in the 'modeling and results' section, the model does not account, so far, for the loss of mass due to overflows. Therefore, the model appears to reproduce well the initial formation and the growth of pulses, providing insights into the onset of the overflow process, but cannot be used to infer the behavior of the pulse *after* the occurrence of an overflow.

It is interesting to discuss the FLOWPULSE simulations with respect to the real scenario and hence to the rheological properties of lava. While in the presented results growing pulses are the effect of thickening of "physically" equivalent parcels, in the real channelized flow, at the same distance from vent, faster volumes of lava are basically hotter than the slower ones, having been exposed to the subaerial environment for less time. For the same reason, faster volumes of lava are also less dense (because of reduced lava outgassing) and less viscous than the slower ones (as a combined effect). As a result, during the thickening process, the contrast in physical and rheological properties of lava within clustering parcels is greater for higher initial values of a_v and for longer times after emission from the vent.

Even though the presented model does not take into account any specific flow structure (e.g. laminar flow), we assume that FLOWPULSE can still capture the broad dynamics of a pulsating flow, and we discuss the results with respect to the actual laminar structure of lava flows (e.g. Harris 2013; Filippucci et al. 2013). In the vertical structure of a growing pulse, the young, hot, less dense and faster lava coming from the rear (especially if a relatively steep slope aids lava motion) will tend to flow over the top of the preceding older, colder and slower lava. Hence, the laminar structure of a pulse will tend to assume not only the usual velocity stratification, but also a thermal layering which is otherwise essentially absent in a lava flow supplied at a steady rate (Filippucci et al. 2013).

The evidence that younger, hotter lava overrides the older, colder one, becomes visually apparent in the progression of a pulse through a distal sector imaged by James et al. (2007). By comparing the different frames of their Fig. 5 (James et al. 2007), it is evident that, beyond overflowing over both levees, the pulse overrides the slower,

thin and colder flow in the channel in front of its snout. In sectors of the channel where thinning occurred, such as the latter one before being overridden by the pulse, the thickness of the flowing lava can attain a minimum which causes a Bingham flow to come to a halt (e.g. Tallarico and Dragoni 1999, 2000), and the thick crustal carapace, developed during slow motion downhill and no longer supported by a much-thinned underlying molten layer, could be pushed to the channel floor by the overriding thick pulse.

A similar mechanism can contribute to progressively raising the bottom of the channel (Fig. 5), supporting the outlined growth dynamics and the formation of perched flow units (Tarquini et al. 2012). Interestingly, Krauskopf (1949) described a similar growth of the lava channels formed at some stage in the winter of 1945-46 during the 1943-52 eruption at Paricutin (Mexico): "*the most curious change in the channels is their gradual building up to a considerable height above the surroundings, much as a river channel confined by levees is built up as the stream drops sediments in its bed*" (Krauskopf, 1949). The same author highlighted that Perret (1924) documented a similar dynamics during the 1906 eruption at Vesuvius. The same growth dynamics have thus been observed in channelized flows formed by a trachybasaltic lava (Etna 2004, Burton et al., 2005), a basaltic-andesitic to andesitic lava (Paricutin, Pioli et al. 2008) and a phono-trephritic lava (Vesuvius 1906, Principe et al. 2004). Krauskopf (1949) further noted that at Paricutin in 1945-46 "*within its channel the level of a flow commonly fluctuates through a vertical range of 1 or 2 meters*" Krauskopf (1949). This fluctuation in flow level suggests a pulsating behavior, and further downflow the moderate fluctuation described above (1-2 m) could have exceeded a superelevation threshold triggering the overflow process (e.g. see Fig. 9). As such, it is possible that, even in the described scenario at Paricutin, channel growth was promoted by the same iterative overflow as outlined here.

The velocity and thermal stratification favored by the growth of pulses described above suggests that the first lava to spill out from the channel during the overflow would be the shallowest layer (the top of the pulse) composed of the younger, hotter and less viscous lava coming from the rear. In contrast, the older, slower and somewhat cooler lava at the base (near the channel floor) will continue to flow inside.

Due to the slower velocity of the basal layer of the flow with respect to the shallower layers constituting the bulk of a pulse, the basal layer will remain behind after the pulse passes, to become (again) a slow inter-pulse sector in which thinning can facilitate further cooling and where the conditions to "*drop sediments in the bed*" (Krauskopf, 1949) are favored.

An interesting picture emerges from the above, in which a pulse-fed channel grows by layering hot batches of younger lava on the levees while the bottom of the channel is resurfaced with colder blankets of older lava.

This pulsating dynamic in the channel is modeled in FLOWPULSE through a variation in the flux from the vent. As such, the origin of pulses should be somewhere in the feeding system prior to magma's arrival at ("upstream from") the vent, as suggested by several authors (James et al. 2007; Favalli et al. 2010; Wadge et al. 2012). Nevertheless, the movement of lava in an open channel is always affected by other specific mechanisms which have a definite subaerial origin. For example, Bailey et al. (2006) documented flux variations (including the onset of lava surges) caused by the formation and subsequent collapse of channel blockages. Although effusive eruptions are usually the least energetic and the least destructive among volcanic paroxysms, mechanical failures of portions of levees near the vent/crater are very common during lava flow emplacement (Guest et al. 1987; Lipman and Banks, 1987; Calvari and Pinkerton, 2002; Bailey et al., 2006), and partial or total blockages of channels caused by the stacking of rafted down blocks are also common.

In the scenario considered here, it is interesting to note the presence of an anomalous morphological bulge just in front of the overflow point "I " (Figs. 5 and 12). This bulge may suggest that the main channel could have been blocked by the stranding of large blocks (forming the bulge) which caused lava to back up behind them. This blockage would have triggered the initial spill of lava from both sides (which explains the presence of overflow units 1.1. and 1.2). The close-up in the overflow point (Fig. 12), further suggests that, after a short time (because flow unit 1.1 is very small), the right-hand levee experienced a partial collapse which drained the whole flux towards flow unit 1.2, which was the sole active branch at the time of the LIDAR survey and later on 16 September, as shown before.

According to the above discussion, the model presented can successfully explain the growth mechanism of lava units emplaced by pulsating flows and the conditions favoring the onset of channel overflow, but cannot determine, in detail, the overall dynamics and the evolution of a compound lava flow field (including flow bifurcation and branching, levee breaching, etc.) which seems to be driven by an interplay between systematic (i.e. predictable) and non-predictable processes.

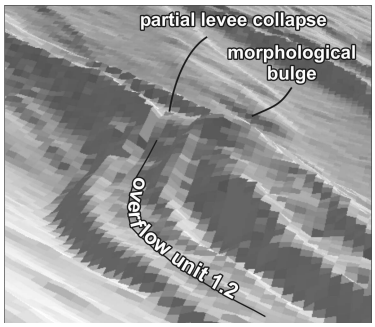

Fig. 12. Close-up of the overflow point highlighting the presence of a morphological bulge just down-channel from the overflow point. It appears that the right-hand levee has been partially dismantled by the breaching lava, facilitating the drainage towards flow unit 1.2.

Conclusion

A systematic, overflow-driven, growth mechanism for lava flow units fed by a pulsating supply is proposed and explained in detail through the analysis of the morphometry of lava channels which were active during an early phase of the 2004-2005 flank eruption at Mount Etna. A simple analytical model (FLOWPULSE) shows that a small fluctuation in the velocity of extrusion of lava propagates down-channel as pulses producing increasingly strong fluctuations in flow depth (upwards and downwards), which eventually result in overflows at given distances from the vent. The simulated behavior captures the outlined growth mechanism, which expands on the original concept of "overflow levees" introduced by Sparks et al. (1976).

The model presented does not directly deal with the inner physical modifications of flowing lava, nor does it explore what happens to a pulse during and after an overflow, and improvements in these areas are possible. Nevertheless, FLOWPULSE simulates, for the first time, the behavior of lava channels fed by a pulsating supply. It shows that a fluctuating supply, in the case presented here, promotes a systematic thickening of intermediate sectors of flow units, supporting the substantial "loss" of the original flowing mass with increasing distance from the vent (James et al. 2007). A similar growth dynamic has previously been documented at other volcanoes in channelized flows formed by lavas having different compositions, suggesting that a unifying, fluctuation-driven process is responsible for the growth of lava channels. By subtracting lava from the flux before it reaches the advancing front, this dynamic slows the flow progression downhill, affecting the maximum distance reached by a channelized lava flow. In particular, for the same average supply rate and same average initial velocity, a higher fluctuation (i.e. higher values of σ_v) causes a higher density of pulses per unit length and an earlier onset of overflow (i.e. closer to the vent, e.g. see Fig. 9), resulting in greater loss of mass from the channel, and hence in a shorter advancement of the lava flow front for the same emplacement duration (widening is favored instead of lengthening).

Acknowledgments

Max Favalli and Ale Fornaciai are acknowledged for having shared some LIDAR-based topographic measurements. Sonia Calvari and Bob Wright are acknowledged for having provided details of the time of acquisition of the thermal map and Hyperion scenes (respectively). Francesco Mazzarini and three anonymous reviewers provided useful comments to an early version of the manuscript. Two anonymous reviewers, the associated editor M.R. Patrick and the executive editor J.D.L. White improved the final version of the paper.

Appendix

Assuming a constant flux throughout the whole channel, a velocity decay $\tilde{v}$ for the reference steady solution is defined as a function of the flow depth h and the flow width w. If we assume a linear increase with the distance x from the vent:

$$w = w_0 + w_x x$$

$$h = h_0 + h_x x$$

where w_0 and h_0 are the width and the height of the flow at the vent respectively and w_x and h_x are constant parameters (see main text), the velocity decay can be expressed as

$$\tilde{v} = \tilde{v}(x) = \frac{w_0 h_0}{w(x)h(x)} = \frac{w_0 h_0}{(w_0 + w_x x)(h_0 + h_x x)}.$$

When the steady supply is varied, the initial velocity v_0 of each parcel becomes a function of the emission time t_0, and the velocity of an parcel at a distance x from the vent and emitted at time t_0 is

$$v(x,t_0) = v_0(t_0)\tilde{v}(x).$$

Now, being $v = \frac{dx}{dt}$, integrating the expression of the velocity we obtain

$$\int_{t_0}^{t} dt = \int \frac{1}{v(x,t_0)} dx \quad t - t_0 = V(x)$$

where $V(x,t_0)$ is a primitive of the reciprocal of the velocity v. If we denote with W the inverse function with respect to x of $V(x,t_0)$, then we can express explicitly the position x of any parcel given the actual time t and the emission time t_0 as

$$x = W(t,t_0).$$

In order to introduce the interaction between the parcels, we first observe that differentiating W with respect to t we obtain the velocity of the parcels as a function of the time t and the emission time t_0:

$$v = \frac{dx}{dt} = \frac{dW}{dt} = W_t(t,t_0)$$

and the distance x can be written as

$$x(t,t_0) = x_0 + \int_0^t W_t(s,t_0)\,ds \qquad \text{(A1)}$$

If we introduce now an interaction of the parcels, assuming that the velocity of an parcel emitted at time t_0 is controlled also by the velocity of the parcels emitted in the time interval $[t_0-\Delta t_0;\ t_0+\Delta t_0]$ through a convolution kernel g (for example a Gaussian or square function), a modified velocity can be expressed as

$$W_t^{conv}(t,t_0) = \int_{t_0-\Delta t_0}^{t_0+\Delta t_0} W(t,\eta)\,g(t-\eta)\,d\eta$$

and the resulting distance from the vent at time t is

$$x^{conv}(t,t_0) = x_0 + \int_0^t W_t^{conv}(s,t_0)\,ds = x_0 + \int_0^t \int_{t_0-\Delta t_0}^{t_0+\Delta t_0} W(s,\eta)\,g(s-\eta)\,d\eta\,ds \qquad \text{(A2)}$$

The solutions obtained with a steady supply and with a fluctuating supply with and without convolution applied are presented in Figs. 7-10.

References

Bailey JE, Harris AJL, Dehn J, Calvari S, Rowland SK (2006) The changing morphology of an open lava channel on Mt. Etna. Bull Volcanol 68:497–515

Baloga S (1987) Lava flows as kinematic waves. J Geophys Res 92:B9 9271–9279

Burton MR, et al (2005) Etna 2004–2005: an archetype for geodynamically-controlled effusive eruptions. Geophys Res Lett 32:L09303. doi:10.1029/2005GL022527

Calvari S, Pinkerton H (2002) Instabilities in the summit region of Mount Etna during the 1999 eruption. Bull Volcanol 63:526–535

Favalli M, Fornaciai A, Pareschi MT (2009) LIDAR strip adjustment: application to volcanic areas. Geomorphology 111:123–135

Favalli M, Fornaciai A, Mazzarini F, Harris AJL, Neri M, Behncke B, Pareschi MT, Tarquini S, Boschi E (2010) Evolution of an active lava flow field using a multitemporal LIDAR acquisition. J Geophys Res 115:B11203. doi:10.1029/2010JB007463

Filippucci M, Tallarico A, Dragoni M (2013) Role of heat advection in a channeled lava flow with power-law temperature dependent rheology. J Geophys Res 118:2764–2776. doi:10.1002/jgrb.50136

Frazzetta G, Romano R (1984) The 1983 Etna eruption: Event chronology and morphological evolution of the lava flow. Bull Volcanol 47:1079–1096

Guest JE, Kilburn CRJ, Pinkerton H, Duncan AM (1987) The evolution of lava flow-fields: Observations of the 1981 and 1983 eruptions of Mount Etna, Sicily. Bull Volcanol 49:527–540

Harris AJL, Rowland SK (2001) FLOWGO: a kinematic thermo-rheological model for lava flowing in a channel. Bull Volcanol 63:20–44

Harris AJL, Bailey J, Calvari S, Dehn J (2005) Heat loss measured at a lava channel and its implications for down-channel cooling and rheology. Geol Soc Am Spec Pap 396:125–146

Harris AJL, Favalli M, Mazzarini F, Pareschi MT (2007) Best-fit results from application of a thermo-rheological model for channelized lava flow to high spatial resolution morphological data. Geophys Res Lett 34:L01301. doi:0.1029/2006GL028126

Harris AJL (2013) Lava flows. In: Fagents SA, Gregg TKP, Lopes RMC (eds) Modeling volcanic processes: the physics and mathematics of volcanism. Cambridge University Press, New York, pp 85–106

Hulme G (1974) The interpretation of lava flow morphology. Geophys J R Astron Soc 39:361–383

James MR, Pinkerton H, Robson S (2007) Image based measurement of flux variation in distal regions of active lava flows. Geochem Geophys Geosyst 8:Q03006. doi:10.1029/2006GC001448

James MR, Pinkerton H, Ripepe M (2010) Imaging short period variations in lava flux. Bull Volcanol 72:671–676

Krauskopf KB (1948) Lava movement at Paricutin Volcano,Mexico. Geol Soc Am Bull 59:1267-1284

Lautze NC, Harris AJL, Bailey JE, Ripepe M, Calvari S, Dehn J, Rowland S (2004) Pulsed lava effusion at Mount Etna during 2001. J Volcanol Geotherm Res 137:231–246

Lipman PW, Banks NG (1987) Aa flow dynamics, Mauna Loa. In: Decker W, Wright TL, Stauffer PH (eds) Volcanism in Hawaii. US Geol Surv Prof Paper no. 1350, pp 1527–1567

Mazzarini F, Pareschi MT, Favalli M, Isola I, Tarquini S, Boschi E (2005) Morphology of basaltic lava channels during the Mt. Etna September 2004 eruption from airborne laser altimeter data. Geophys Res Lett 32:L04305. doi:10.1029/2004GL021815

Naranjo JA, Sparks RSJ, Stasiuk MV, Moreno H, Ablay GJ (1992) Morphological, structural and textural variations in the 1988–1990 andesite lava of Lonquimay Volcano. Chile. Geol Mag 129:657–678

Perret FA (1924) The Vesuvius eruption of 1906, study of a volcanic cycle. Carnegie Inst. Washington Pub 339, 151 pp

Pioli L, Erlund E, Johnson E, Cashman K, Wallace P, Rosi M, Delgado Granados H (2008) Explosive dynamics of violent Strombolian eruptions: The eruption of Parícutin Volcano 1943–1952 (Mexico). Earth Plan Sci Lett 271:359-368

Principe C, Tanguy JC, Arrighi S, Paiotti A, Le Goff M, Zoppi U (2004) Chronology of Vesuvius activity from A.D. 79 to 1631 based on archeomagnetism of lavas and historical sources. Bull Volcanol 66:703–724

Robertson JC, Kerr RC (2012) Isothermal dynamics of channeled viscoplastic lava flows and new methods for estimating lava rheology. J Geophys Res 117:B01202. doi:10.1029/2011JB008550

Sparks RSJ, Pinkerton H, Hulme G (1976) Classification and formation of lava levee on Mount Etna Sicily. Geology 4:269–271

Tallarico A, Dragoni M (1999) Viscous Newtonian laminar flow in a rectangular channel: application to Etna lava flows. Bull Volcanol 61:40–47

Tallarico A, Dragoni M (2000) A three-dimensional Bingham model for channeled lava flows. J Geophys Res 105 B11:25,969–25,980

Tarquini S, Favalli M, Mazzarini F, Isola I, Fornaciai A (2012) Morphometric analysis of lava flow units: case study over LIDAR-derived topography at Mount Etna, Italy. J Volcanol Geotherm Res 235–236:11–22

Wadge G, Saunders S, Itikarai I (2012) Pulsatory andesite lava flow at Bagana Volcano. Geochem Geophys Geosyst 13:Q11011. doi:10.1029/2012GC004336

Wright R, Garbeil H, Davies AG (2010) Cooling rate of some active lavas determined using an orbital imaging spectrometer. J Geophys Res 115:B06205. doi:10.1029/2009JB006536